

# Silicone-Based Cholesteric Liquid Crystalline Polymers: Effect of Crosslinking Agent on Phase Transition Behavior

Rabindranath N. Jana,<sup>1</sup> Jae Whan Cho<sup>2</sup>

<sup>1</sup>Artificial Muscle Research Center, Konkuk University, Seoul 143-701, Korea

<sup>2</sup>Department of Textile Engineering, Konkuk University, Seoul 143-701, Korea

Received 3 November 2008; accepted 17 June 2009

DOI 10.1002/app.31021

Published online 12 August 2009 in Wiley InterScience (www.interscience.wiley.com).

**ABSTRACT:** Silicone-based cholesteric liquid crystalline polymers (ChLCP) were fabricated with variable clearing temperatures as controlled by their chemical compositions. The chemical structures of the mesogenic monomers and ChLCP were confirmed by FTIR and <sup>1</sup>H-NMR spectroscopy. The mesogenic properties and phase behavior were investigated by differential scanning calorimetry, polarizing optical microscopy, and X-ray diffraction measurements. The experimental results demonstrated that the glass transition temperatures and the clearing points of the liquid crystalline polymers decreased with increasing pro-

portion of mesogenic crosslinking agent up to 12.50 mol % (LCP-3), and at higher proportion of crosslinking agent, the clearing points disappeared, indicating that the network chains have less chance to orient themselves. Thermogravimetric analysis showed that the LCP-3 was the most stable up to 230°C. © 2009 Wiley Periodicals, Inc. *J Appl Polym Sci* 114: 3566–3573, 2009

**Key words:** liquid-crystalline polymers; crosslinking; thermal properties

## INTRODUCTION

Cholesteric liquid crystal polymers (ChLCP) have been attracted a considerable attention because of their excellent optical properties such as selective reflection of light, thermochromism, and circular dichroism.<sup>1–4</sup> They possess many important applications in various areas such as ink and paint industries, flat-panel displays, thermal imaging, nonlinear optical devices, rewritable full-color image recording, and photostable UV screens.<sup>5–17</sup> The crosslinked ChLCP are also available to some specific optical applications because of their helical structures of the cholesteric phase which may be permanently fixed so that the optical properties become temperature independent.<sup>18,19</sup> Moreover, lightly crosslinked ChLCP may show the basic features of polymeric elastomers with anisotropic physical properties coming from their cholesteric liquid crystal phases with reversible phase transition during heating and subsequent cooling.<sup>20,21</sup> Besides their electro-optical and mechanical properties, ChLCP may show piezoelectric properties arising from the deformation of helical structure of the cholesteric phase.<sup>22–25</sup> The helical structure and the pitch of cholesteric liquid crystal-

line polymers are dependent on the temperature and concentration of the chiral constituents.<sup>26</sup> The pitch can be fixed either by formation of suitable polymer architectures or simply by formation of polymer network to stabilize the cholesteric structure.<sup>27</sup> However, it is important to study how the crosslink units change the helical structure of cholesteric phase and the pitch of the liquid crystalline phases of the ChLCP. Zhang et al.<sup>28</sup> studied the effect of ionic crosslinks on phase transition behavior of silicone-based cholesteric liquid crystalline polymer. It was found that the sample with more ionic mesogens displayed smectic and cholesteric mesophase. With an increase of ionic groups in the polymers, the glass transition temperature and clear point change a little, and the enthalpy changes of melt increase with an increase of ionic content of the polymers. The effect of spacer length on liquid crystal properties has been also reported,<sup>29</sup> and with an increase of the number of methylene units in the side chains of the polymers, there was an increase in the layer spacing values for the cholesteric liquid crystalline phases. That layer spacing represented the thickness of the neighboring twisted layers in a helical structure. Based on the significant shift of the maximum reflection peak for the liquid crystalline phases, the pitch distance in the helical structure also increased with an increase in the length of methylene units in the side chains.

In this study, 1,4-butanediol diundecylenate based flexible crosslinking agent (M-1) and cholesterol based mesogenic monomer (M-2) were synthesized

Correspondence to: J. W. Cho (jwcho@konkuk.ac.kr).

Contract grant sponsor: Korea Research Foundation; contract grant number: KRF-2006-005-J03302.

and then introduced simultaneously into the polyhydrosiloxane chain. Here we have used a highly flexible polysiloxane as an LCP backbone. This is because (i) glass transition temperature ( $T_g$ ) can be reduced to get better flexibility of the polymers, (ii) for cholesteric LCP, a helical conformation is important, and so a flexible backbone is necessary, and (iii) the flexible backbone may allow crystallization of the cholesterol molecules pendent to the backbone of the LCP [21]. The aim of this work is to investigate the effect of the crosslinking agent on the phase transition behavior of the liquid crystalline polymers synthesized. The mesomorphic properties of the monomer and polymers obtained were characterized with an investigation of their phase transition behavior.

## EXPERIMENTAL

### Materials

Polymethyl hydrosiloxane (PMHS,  $n = 35$ ) with  $M_n$  1,700–3,200, refractive index  $[n]_D^{20}$  1.398, density 1.006 g/mL; 10-undecenoic acid with mp 23–25°C, bp 137°C and density 0.912 g/mL; allyl bromide with mp 119°C, bp 70–71°C, and density 1.398 g/mL, containing 300 ppm propylene oxide as stabilizer; hexachloroplatinic acid ( $H_2PtCl_6$ ) (8 wt % in water) with density 1.05 g/mL and cholesterol (99% pure) with mp 147–149°C, bp 360°C, density 1.067 g/mL, were purchased from Sigma-Aldrich. 1,4-butanediol was supplied by Junsei Chemicals, Japan. All other chemicals were of LR grade reagents.

### Characterization

Fourier transform infrared (FTIR) spectroscopic measurements were performed using a Jasco FTIR 300E with an attenuated total reflectance method.  $^1H$ -NMR characterizations were performed using a Bruker Advanced DMX 500 spectrometer. The samples were prepared in  $CDCl_3$  at room temperature. DSC experiments were performed on a TA Instruments (Q100) with heating of 10°C/min and cooling rate of 5°C/min in a flowing  $N_2$  atmosphere. The temperatures corresponding to maxima of the DSC endothermic peaks of the second heating traces were assigned as phase transition temperatures i.e., glass transition, melting, and isotropic transition.<sup>30</sup> The midpoint of the heat capacity stepwise increase was taken as the glass transition temperature. Thermogravimetric (TG) and derivative thermogravimetric analysis of the samples were carried out in a thermogravimetric analyzer (TGA Q2050) from room temperature to 600°C in nitrogen atmosphere and at heating rate of 10°C/min. Wide-angle X-ray diffraction studies using monochromatized  $CuK_\alpha$  radiation

and a nickel filter were carried out in X-ray diffractometer (Bruker AXS). The diffraction was recorded at a scanning speed of 5°/min. The area ratio of crystalline peaks to the total area of crystalline and amorphous peaks was used as the measure of crystallinity. The crystallite size ( $P_{hkl}$ ) and interchain distance ( $r_{hkl}$ ) were calculated from Scherrer equation,<sup>31</sup>

$$P_{hkl} = K\lambda/\beta \cos \theta \quad (1)$$

$$r_{hkl} = \lambda/2 \sin \theta \quad (2)$$

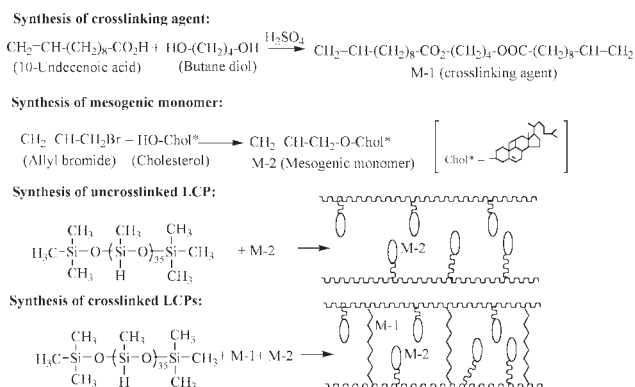
where  $K$  is a Scherrer constant which equals to 0.9,  $\lambda$  wavelength of the radiation (1.54 Å for  $CuK_\alpha$ ),  $\beta$  width of the peak at half maximum, and  $\theta$  angle of incidence. Polarized optical microscope (Eclipse LV 100 POL) from Nikon Corporation, Tokyo, Japan, equipped with a hot stage (LTS 350) from Linkon Scientific Instruments, England, UK, was used to observe visual textures and phase transition temperatures for analyzing the mesomorphic properties of the liquid crystalline monomers and polymers. The samples used for POM analysis were sandwiched between two glass cover slips and melted on a hot stage at 250°C, care being taken to avoid cover slip sliding over that would lead to void formation, and subsequently cooled to room temperature. The temperature ramping rates were chosen to be consistent with DSC experiments for comparison purposes.

### Synthesis of crosslinking agent (M-1)

Undecylenic acid 22.08 g (0.12 mol) and 5.9 g (0.05 mol) of 1,6-hexanediol were dissolved in 30 mL benzene, and then 1 mL concentrated sulfuric acid was added. After the mixture was mixed uniformly, it was refluxed at 80°C for 8 h, and the mixture was poured into 200 mL of water. After removing the water layer, the oil layer was neutralized with 2%  $NaHCO_3$  to pH 7, washed several times with distilled water, and dried with  $Na_2SO_4$ . Then the distillate of crude product, collected at 175°C under 3 mmHg pressure gave the transparent liquid (Scheme 1).

### Synthesis of mesogenic monomer (M-2)

Cholesterol [19.3 g (0.05 mol)] was dissolved in 80 mL of chloroform, followed by the dropwise addition of 30 mL of an aqueous solution of potassium hydroxide (30 wt %), and then 6.0 g (0.05 mol) allyl bromide was slowly dropped into the mixture. After the mixture was reacted at room temperature for 2 h and was refluxed at 90°C for 4 h, it was cooled to room temperature and poured into 300 mL of deionized water to form a transparent yellow solution. An organic phase was then extracted with 50 mL of



**Scheme 1** Synthesis of crosslinking agent, mesogenic monomer, and LCPs.

diethyl ether three times. To the aqueous phase, 80 mL of 30% hydrochloric acid solution was added, leading to the precipitation of the desired product. The precipitate, a white solid, was collected after filtration and further recrystallized from ethanol (Scheme 1).

### Synthesis of LCP

LCPs were prepared by a graft reaction, in which the crosslinking agent M-1 (except for LCP-0) and the mesogenic monomer M-2 were simultaneously attached to the highly flexible polysiloxane via a hydrosilation reaction. The monomers M-1, M-2, and PMHS were dissolved in dry toluene (Table I). The reaction mixture was heated to 65°C under nitrogen, and then 2 mL of 0.5%  $\text{H}_2\text{PtCl}_6/\text{THF}$  catalyst solution was injected. The reaction was kept at 65°C under nitrogen until the Si-H absorption peak of PMHS at 2160  $\text{cm}^{-1}$  disappeared. It took about 12 h to complete the reaction. Then the elastomers were carefully deswollen with methanol and dried under vacuum (Scheme 1).

## RESULTS AND DISCUSSION

### FTIR and Raman analysis

FTIR spectra of the crosslinking agent (M-1), mesogenic monomer (M-2) and LCP-1 at the initial stage and after 12 h of reaction are presented in Figure 1.

**TABLE I**  
Composition of Samples Synthesized in this Study

Sample Code	PMHS (mmol)	M-1 (mmol)	M-2 (mmol)	M-1 (mol%)	Yields (%)
LCP-1	1.00	0.25	5.75	4.16	86
LCP-2	1.00	0.50	5.50	8.33	90
LCP-3	1.00	0.75	5.25	12.50	92
LCP-4	1.00	1.25	4.75	20.83	87
LCP-5	1.00	1.50	4.50	25.00	86

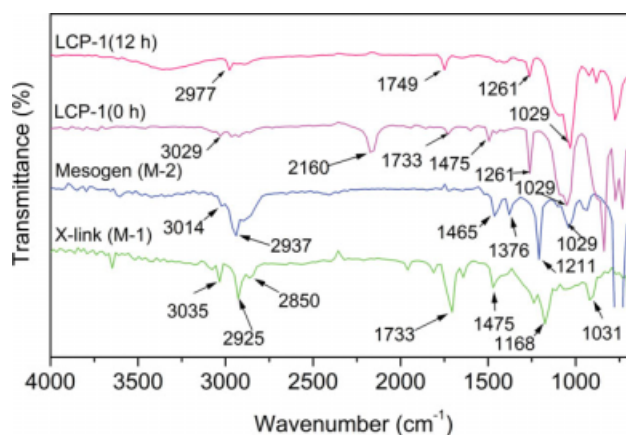


**Figure 1** FTIR spectra of crosslinking agent (M-1), mesogenic monomer (M-2) and liquid crystal polymer (LCP-1) at initial stage (0 h) and after 12 h of reaction. [Color figure can be viewed in the online issue, which is available at [www.interscience.wiley.com](http://www.interscience.wiley.com).]

The FTIR spectra of M-1 shows the characteristic transmittance peaks corresponding to C-H stretching of vinyl at 3035  $\text{cm}^{-1}$ , C-H of methylene at 2925 and 2850  $\text{cm}^{-1}$ , alkane ester group ( $-\text{RCOOR}-$ ) at 1733  $\text{cm}^{-1}$  and C=C of vinyl at 1475  $\text{cm}^{-1}$ .<sup>21,32</sup> The cholesteric monomer (M-2) shows characteristic transmittance peaks corresponding to C-H stretching of vinyl at 3014  $\text{cm}^{-1}$ , C-H of methylene at 2937  $\text{cm}^{-1}$ , C=C of vinyl at 1465 and 1376  $\text{cm}^{-1}$  and C-O-C at 1211 and 1029  $\text{cm}^{-1}$ . FTIR spectra of network liquid crystalline polymers formed after 12 h reaction show the complete disappearance of the peaks for the Si-H stretching at 2160  $\text{cm}^{-1}$  of PMHS and vinyl C=C stretching at about 1475  $\text{cm}^{-1}$  and 1465  $\text{cm}^{-1}$  of the x-linking agent (M-1) and mesogenic monomer (M-2), respectively.<sup>21,32</sup> This is only possible if the vinyl groups of M-1 and/or M-2 react with the Si-H group of PMHS. Thus it is concluded that the crosslinking agent (M-1) and mesogenic monomer (M-2) have been successfully incorporated into the polysiloxane chain.

The structure for the crosslinking agent, mesogen and LCPs was also confirmed from  $^1\text{H-NMR}$  analysis. The different chemical shifts as observed; 5.73 (4H, m), 5.75 (2H, m), 4.86 (4H, t), 2.27–1.31(16H, t),

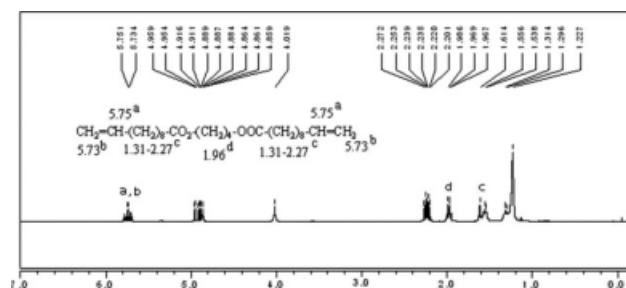


**Figure 2**  $^1\text{H-NMR}$  of crosslinking agent (M-1).

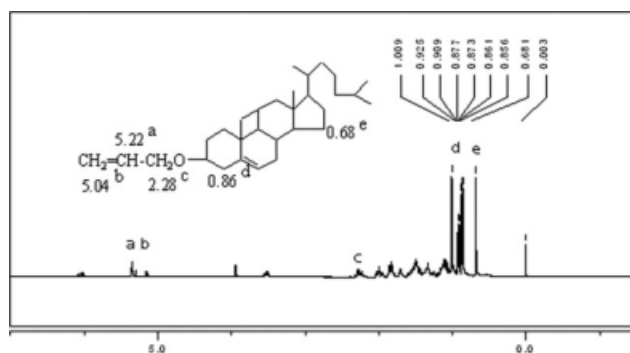


Figure 3  $^1\text{H-NMR}$  of mesogenic monomer (M-2).

1.98 (4H, m) clearly indicated the formation of crosslinking agent<sup>33</sup> (Fig. 2). Similarly, mesogen has the chemical shift of 5.04 (2H, m), 5.92 (1H, m), 2.28 (2H, t), 0.86 (6H, m), 0.68 (2H, m) (Fig. 3). LCP has a new shift at 1.55 (2H, m) which is due to the methyl hydrogen coming from Si-CH<sub>2</sub> bond formation (Fig. 4).

#### Effect of crosslinking agent on phase transition behavior

The liquid crystalline phase transition behavior of network polymers was determined by DSC. The LCP-0 to LCP-3 revealed the glass transition at low temperature near 35 to 40°C and isotropic transition at high temperature near 210°C (Fig. 5). However, LCP-4 and LCP-5 only showed the  $T_g$  at low temperature near 35°C and no liquid crystalline to isotropic transition temperature ( $T_i$ ) due to high crosslink density.<sup>21</sup> The corresponding phase transition temperatures and enthalpy changes of the isotropic transition are given in Table II. It is found that the  $T_g$  values of LCP-2 and LCP-3 are slightly higher than that of LCP-0, this is due to the presence of crosslinks in the polymers. Afterwards, the  $T_g$  of the crosslinked LCPs is shifted to a lower value. This is because, for side-chain ChLCP,  $T_g$  tends to be influ-

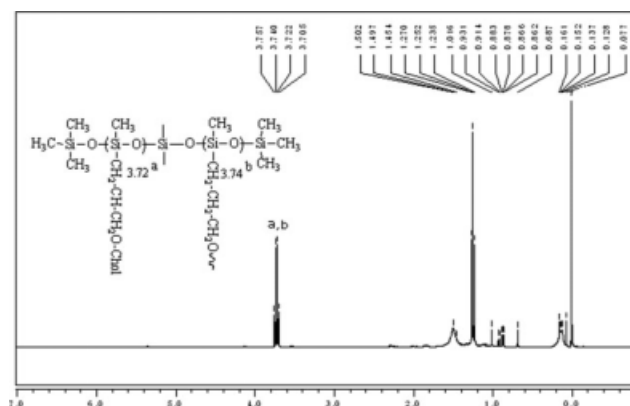


Figure 4  $^1\text{H-NMR}$  of LCP-1.

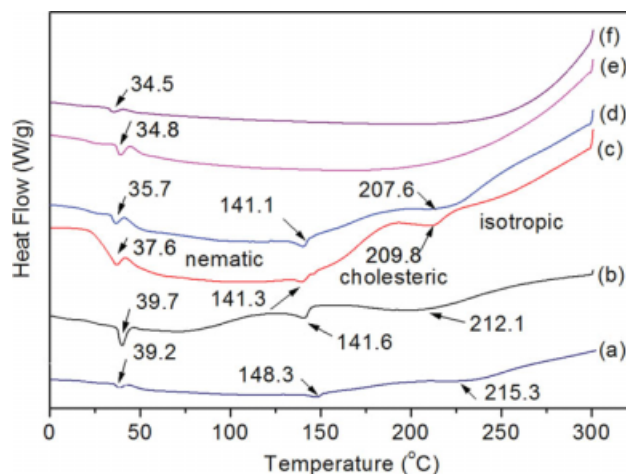


Figure 5 DSC traces of different liquid crystal polymers (a) LCP-0, (b) LCP-1, (c) LCP-2, (d) LCP-3, (e) LCP-4, and (f) LCP-5. [Color figure can be viewed in the online issue, which is available at [www.interscience.wiley.com](http://www.interscience.wiley.com).]

enced by the polymer backbone, mesogenic group, flexible spacer length, and crosslinking density. The chemical crosslinking imposes additional constraints on the motion of chain segments, and thus makes  $T_g$  increase. On the other hand, the flexible chain of the crosslinking agent similar to the plasticization may cause  $T_g$  to decrease. Because of flexible chains in both ends of the crosslinking agent for the synthesized polymers, the plasticization of flexible chains is much more significant than the crosslinking limitation on the motion of chain segments.<sup>21</sup> So, with the increasing concentration of crosslinking agent from 4.16 to 25.00 mol %,  $T_g$  decreased from 39.7°C for LCP-1 to 34.5°C for LCP-5. As the density of crosslinking (M-1) units increased from 4.16 to 12.50 mol %,  $T_i$  reduced from 212.1°C for LCP-1 to 207.6°C for LCP-3, and  $T_i$  of LCP-4 and LCP-5 disappeared due to high crosslinking density. At high crosslink density, the plasticizing effect of the flexible chain of the crosslinking agent on  $T_i$  of liquid crystalline elastomers becomes minor. The transition near 210°C is speculated as due to the phase change from cholesteric liquid crystalline to isotropic liquid crystal structure which is confirmed from phase morphology studies (discussed later). The temperature between  $T_g$  and  $T_i$  is the mesogenic range ( $\Delta T$ ) of the polymers. From Table II, it can be seen that the crosslinking agent leads to a parallel downshift of  $T_g$  and  $T_i$ , so,  $\Delta T$  change is very little. The enthalpy changes ( $\Delta H$ ) decreased from 2.35 Jg<sup>-1</sup> for LCP-1 to 1.53 Jg<sup>-1</sup> for LCP-3. Thus in the liquid crystal range, LCP-0 to LCP-3 revealed elasticity and reversible phase transitions on heating and cooling cycles. Liquid crystalline type and texture did not change when the concentration of the crosslinking unit was less than 12.50 mol %. Whereas, LCP-4 and LCP-5 with 20.83 and 25.00 mol % of crosslinking

TABLE II  
DSC and POM Results of polymers Used in this Study

Sample Code	DSC					POM	
	$T_g$ (°C)	$T_m$ (°C)	$T_i$ (°C)	$\Delta H$ (J/g)	$\Delta T$ (°C)	$T_{cl}$ (°C)	$T_{lc}$ (°C)
LCP-0	39.2	148.3	215.3	1.50	176.1	213	212
LCP-1	39.7	141.6	212.1	2.35	172.4	210	209
LCP-2	37.6	141.3	209.8	1.75	172.2	209	208
LCP-3	35.7	141.1	207.6	1.53	171.9	208	206
LCP-4	34.8	–	–	–	–	–	–
LCP-5	34.5	–	–	–	–	–	–

$T_g$ , glass transition temperature;  $T_m$ , melting temperature;  $T_i$ , isotropic transition temperature;  $\Delta H$ , enthalpy of crystallization;  $\Delta T$ , mesogenic temperature range ( $T_i - T_g$ );  $T_{cl}$ , temperature at which the birefringence disappeared completely;  $T_{lc}$ , temperature at which the mesogenic phase occurred.

agents, respectively, did not show any texture due to high crosslink density.

### Effect of crosslinking agent on thermal stability

The TGA scans for the LCPs are shown in Figure 6. Thermal stability of the ChLCP increases initially with increasing a proportion of crosslinking agent up to 12.50 mol % (LCP-3) and then it decreases (Table III). For instance, the values of  $T_{10}$ , the temperature at which 10% of the materials has been degraded, for LCP-0 to LCP-5 are 405, 420, 452, 501, 269, and 199°C, respectively. The maximum degradation temperatures ( $T_{1max}$ ,  $T_{2max}$ ), the temperatures at which the degradation shows the peak maximum, and temperature of finish ( $T_f$ ), the temperature after which no appreciable degradation of the materials is possible, increase for LCP-0 to LCP-3. Thus the LCP-3 i.e., with 12.50 mol % of crosslinking agent, shows the maximum thermal stability. The increase in thermal stability with the increase of crosslinking agent may be due to the formation of a stable covalent bond between the siloxane chains as shown in the

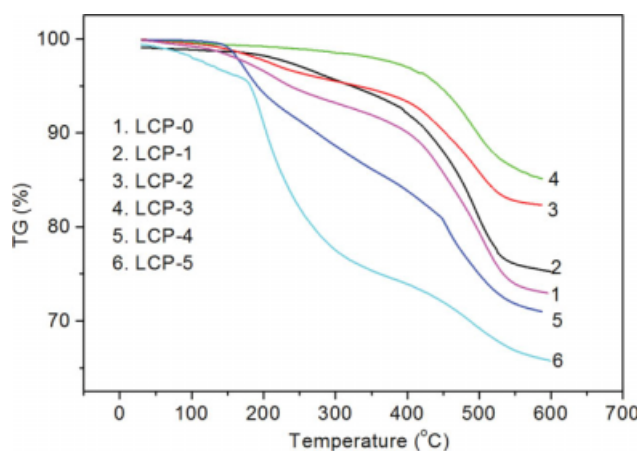


Figure 6 TGA traces of different liquid crystal polymers. [Color figure can be viewed in the online issue, which is available at [www.interscience.wiley.com](http://www.interscience.wiley.com).]

Scheme 1. At higher proportion (>12.50 mol %) of crosslinking agent i.e., LCP-4 and LCP-5, the network formed experiences much more strain coming from their highly crosslinked structures, so they even start degrading at around 100°C (Fig. 6). Moreover, the carbonyl group containing crosslinking agent is more susceptible to thermal degradation at high temperature leading to lowering of thermal stability of the polymers with higher crosslinking agent (>12.50 mol %).

### Effect of crosslinking agent on crystallization behavior

XRD measurements were performed to interpret the crystallization behavior of the LCPs. In general, a smectic liquid crystalline phase shows sharp and strong peaks in small angle region, together with a broad peak in wide-angle region.<sup>21</sup> However, nematic and cholesteric liquid crystalline phases only show a broad peak in the wide-angle region.<sup>21</sup> For the network polymers in this study, no peak was found in the small angle region, but the two broad peaks associated with the lateral packing at wide-angle appeared at about  $2\theta = 10.2^\circ$  and  $22.5^\circ$  in wide-angle X-ray diffraction region (Fig. 7). Therefore, it is confirmed that the XRD results are due to the formation of the nematic and cholesteric phase structures for LCP-0 to LCP-3. The degree of crystallinity ( $X_c$ ), crystallite sizes ( $P_{110}$ ,  $P_{200}$ ), size anisotropy ( $P_{110}/P_{200}$ ), and interchain distances of the

TABLE III  
Thermal Stability of Samples Used in this Study

Sample Code	$T_{10}$ (°C)	$T_{1max}$ (°C)	$T_{2max}$ (°C)	$T_f$ (°C)
LCP-0	405	–	491	570
LCP-1	420	–	496	568
LCP-2	452	–	499	572
LCP-3	501	–	499	582
LCP-4	269	174	455	569
LCP-5	199	198	491	559

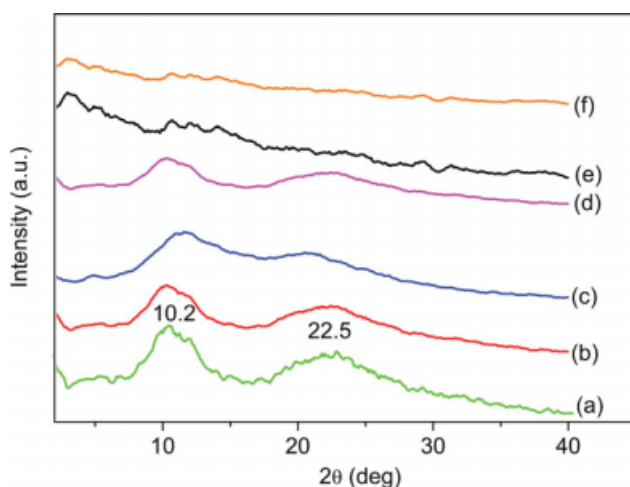


**Figure 7** Wide-angle X-ray diffraction of patterns of different liquid crystal polymers, (a) LCP-0, (b) LCP-1, (c) LCP-2, (d) LCP-3, (e) LCP-4 and (f) LCP-5. [Color figure can be viewed in the online issue, which is available at [www.interscience.wiley.com](http://www.interscience.wiley.com).]

polymers, measured from the X-ray diffraction patterns (Fig. 7) are summarized in Table IV. Thus with the addition of x-linking agent,  $X_c$  decreases regularly. The peaks near  $2\theta = 10.2$  and  $22.5^\circ$  are due to formation of the crystals in two different directions which correspond to (110) and (200) reflections, respectively.<sup>32</sup> The crystallite size in both the directions decreases showing a reduced size anisotropy. The interchain distance ( $r_{110}$ ,  $r_{200}$ ) also gradually decreases with an increase in x-linking agent. The decrease in crystallinity and crystal size with increasing crosslinking agent suggests that the mesomorphic crosslinking agent affects largely on the liquid crystalline order. For LCP-4 and LCP-5, there is no such crystalline peak both in small angle and wide-angle ranges. The high crosslinking leads to the disappearance of isotropic transition of LCP-4 and LCP-5 which is in good agreement with the DSC studies.

#### Effect of crosslinking agent on phase morphology

When the cholesterol was heated to  $147^\circ\text{C}$ , the sample began to melt into a typical cholesteric oily texture, and then a broken focal-conic texture appeared, and the texture disappeared at  $148^\circ\text{C}$ . When the isotropic state was cooled to room temperature, the bright focal-conic texture with selective color reflections from the different planes appeared, as shown in Figure 8(a). It is well known that the helical pitch is an important parameter in connection with structures and optical properties of the cholesteric phase. The pitch and the reflection wavelength depend on the molecular structure, such as the polymers back-

bone, the length of mesomorphic core, flexible spacer length, and intermolecular force and so on.<sup>33</sup>

After heating up to  $250^\circ\text{C}$ , and subsequently cooling to room temperature ( $25^\circ\text{C}$ ) at a cooling rate of  $5^\circ\text{C}/\text{min}$ , it has been observed that the crystals are grown radially with significant branching during cooling [Fig. 8(b,c)]. As LCP-0 to LCP-3 show similar type of phase morphology observed from the POM, for convenience, the phase morphology only for LCP-3 has been reported here in details. POM for LCP-3 [Fig. 8(c)] shows a nematic liquid crystal structure. With a close observation inside into the liquid crystals, it can be seen that the liquid crystals are also arranged in different helicoidal forms, characteristic of cholesteric liquid crystalline polymers. So at room temperature it shows both the nematic and cholesteric textures<sup>34</sup> [Fig. 8(c)]. Now again during second heating as the temperature increases, the nematic phase disappears at about  $142^\circ\text{C}$  and only cholesteric phase [Fig. 8(d)] remains in the texture until the temperature reaches to  $206^\circ\text{C}$  [Fig. 8(e)]. Upon further heating up to  $208^\circ\text{C}$ , it changes into an isotropic liquid [Fig. 8(f)]. So LCP-0 to LCP-3 shows a reversible phase transition on heating and cooling cycles.

But in case of the highly crosslinked liquid crystals, the phase transition behavior is quite different. Again as the POM phase morphology for highly crosslinked liquid crystal polymers (LCP-4 and LCP-5) are similar; the same for only LCP-4 has been reported here. Under the cross polarized light it shows different color reflections from the planes of the liquid crystals [Fig. 9(a)] and the liquid crystals are arranged in a zig-zag way. As the temperature increases, the liquid crystals start melting [Fig. 9(b)] at about  $142^\circ\text{C}$  and it continues up to  $208^\circ\text{C}$  [Fig. 9(c)]. On cooling no proper crystallization is found [Fig. 9(d)], this is because at high level of crosslinking agent ( $>12.50$  mol %) permanent set of the polymer network is possible which restricts the crystallization process. Thus, LCP-4 and LCP-5 do not show complete reversible phase transition on cooling which is consistent with the DSC studies.

**TABLE IV**  
Degree of Crystallinity ( $X_c$ ), Crystallite Size ( $P_{110}$ ,  $P_{200}$ ), Size Anisotropy ( $P_{110}/P_{200}$ ), and Interchain Distances ( $r_{110}$ ,  $r_{200}$ ) of the Polymers

Samples Code	$P_{110}$ (Å)	$P_{200}$ (Å)	$P_{110}/P_{200}$	$r_{110}$ (Å)	$r_{200}$ (Å)	$X_c$ (%)
LCP-0	22.5	12.3	1.82	9.21	4.10	19.2
LCP-1	21.9	12.2	1.79	8.67	3.95	18.5
LCP-2	18.1	10.5	1.72	7.26	3.80	13.9
LCP-3	12.8	8.6	1.49	6.25	3.25	12.3
LCP-4	—	—	—	—	—	—
LCP-5	—	—	—	—	—	—

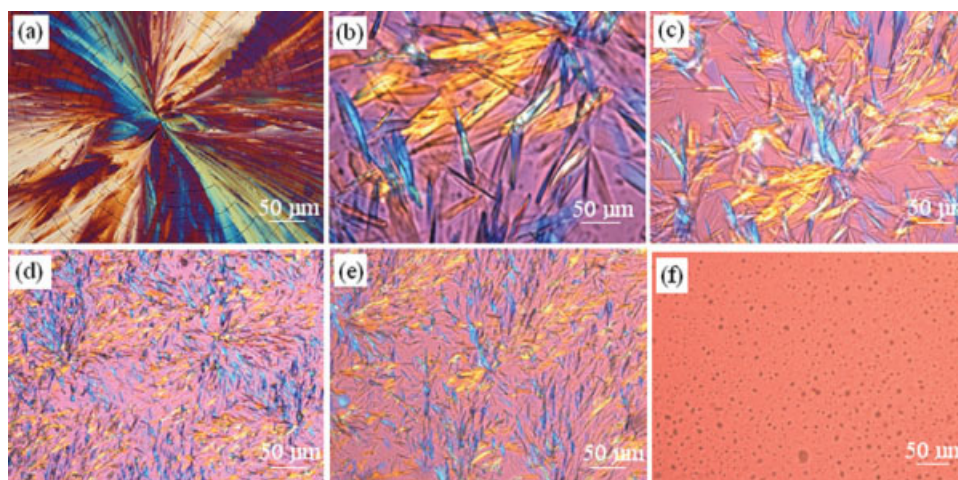


**Figure 8** POM images after first heating and subsequent cooling to 25°C (a) cholesterol, (b) LCP-2, (c) LCP-3; and POM images during second heating for (d) LCP-3, at 142°C, (e) LCP-3, at 206°C, (f) LCP-3, at 208°C. [Color figure can be viewed in the online issue, which is available at [www.interscience.wiley.com](http://www.interscience.wiley.com).]

## CONCLUSION

A series of side-chain liquid crystalline network elastomers containing flexible crosslinking agent and a cholesteric monomer have been synthesized. The structures of the synthesized polymers have been confirmed from FTIR spectroscopy and  $^1\text{H-NMR}$  studies. From DSC studies, it was found that the isotropic transition temperature ( $T_i$ ) decreased with an increase in mesomorphic crosslinking agent. However, the flexible chain of M-1 led to decrease of  $T_g$  values. The liquid crystalline elastomers LCP-0 to LCP-3, containing less than 12.50 mol % crosslinking agents, revealed the elasticity and reversible phase transition on heating and cooling cycles, whereas the highly crosslinked liquid crystal polymers (LCP-4 and LCP-5) did not show such a property. TGA studies showed that the thermal stability of the syn-

thesized polymers increased with the increase in crosslinking agent up to 12.50 mol % of crosslinking agent afterwards it reduced and thus LCP-3 was the most thermally stable. X-ray analysis showed that crosslinking agent affected the liquid crystalline order primarily at high proportion of crosslinking agent. POM studies showed a reversible phase transition for LPC-0 to LCP-3, but not for LCP-4 and LCP-5.

## References

1. Reinitzer, F. *Monatsch Chem* 1888, 9, 421.
2. Du, B. G.; Hu, J. S.; Zhang, B. Y.; Xiao, L. J.; Wei, K. Q. *J Appl Polym Sci* 2006, 102, 5559.
3. Shibaev, V.; Bobrovsky, A.; Boiko, N. *J Photochem Photobio A: Chem* 2003, 155, 3.
4. Liu, J.; Ni, P.; Qiu, D.; Hou, W.; Zhang, Q. *React Funct Polym* 2007, 67, 416.
5. Binet, C.; Ferrère, S.; Lattes, A.; Laurent, E.; Marty, J. D.; Mautzac, M.; Mingotaud, A. F.; Palaprat, G.; Weyland, M. *Analyt Chim Acta* 2007, 91, 1.
6. Bobrovsky, A.; Shibaev, V. *Polymer* 2006, 47, 4310.
7. Bobrovsky, A.; Shibaev, V. *J Photochem Photobio A: Chem* 2005, 172, 140.
8. Shibaev, V.; Bobrovsky, A.; Boiko, N. *Prog Polym Sci* 2003, 28, 729.
9. Bacilieri, A.; Caruso, U.; Panunzi, B.; Roviello, A.; Sirigu, A. *Polymer* 2000, 41, 6423.
10. Freidzon, Y. S.; Boiko, N. I.; Shibaev, V. P.; Plate, N. A. *Eur Polym J* 1986, 22, 13.
11. Broer, D. J.; Lub, J.; Mol, G. N. *Nature* 1995, 378, 467.
12. Bunning, T. J.; Kreuzer, F. H. *Trends Polym Sci* 1995, 3, 318.
13. Yang, D. K.; West, J. L.; Chien, L. C.; Doane, J. W. *J Appl Phys* 1994, 76, 1331.
14. Kricheldorf, H. R.; Sun, S. J.; Chen, C. P.; Chang, T. C. *J Polym Sci Part A: Polym Chem* 1997, 35, 1611.
15. Peter, P. M. *Nature* 1998, 391, 745.
16. Sapich, B.; Stumpe, J.; Krawinkel, T.; Kricheldorf, H. R. *Macromolecules* 1998, 31, 1016.
17. Sun, S. J.; Liao, L. C.; Chang, T. C. *J Polym Sci Part A: Polym Chem* 2000, 38, 1852.

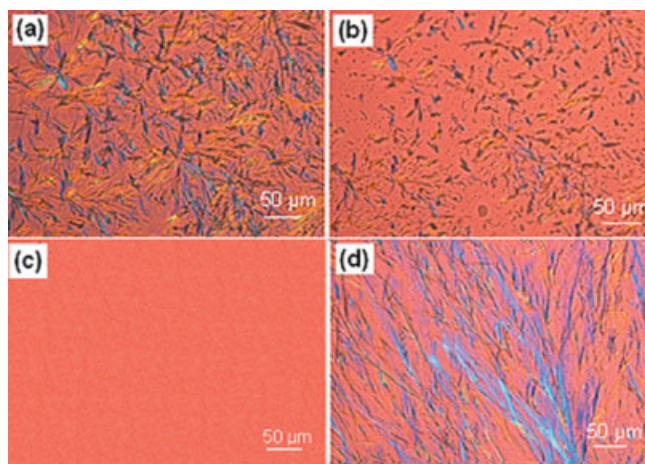


**Figure 9** POM images during first heating of LCP-4 at (a) 25°C, (b) 142°C, (c) 208°C, and (d) 25°C, after cooling. [Color figure can be viewed in the online issue, which is available at [www.interscience.wiley.com](http://www.interscience.wiley.com).]

18. Pfeuffer, T.; Kurschner, K.; Strohsriegl, P. *Macromol Chem Phys* 1999, 200, 2480.
19. Stohr, A.; Strohsriegl, P. *Macromol Chem Phys* 1998, 199, 751.
20. Meng, F.; Zhang, B.; Liu, L.; Zang, B. *Polymer* 2003, 44, 3935.
21. Jia, Y. G.; Zhang, B. Y.; Tian, M.; Wei, K. Q. *React Funct Polym* 2005, 63, 55.
22. Gebhard, E.; Zentel, R. *Macromol Chem Phys* 2000, 201, 902.
23. Mauzac, M.; Nguyen, H. T.; Tournilhac, F. G.; Yablonsky, S. V. *Chem Phys Lett* 1995, 240, 461.
24. Gebhard, E.; Zentel, R. *Macromol Chem Phys* 2000, 201, 911.
25. Kricheldorf, H. R.; Krawinkel, T. *Macromol Chem Phys* 1998, 199, 783.
26. Zhu, J.; Wu, L.; Shi, K.; He, S.; Zhang, P.; Guo, X.; Du, Z.; Zhang, B. *React Funct Polym* 2007, 67, 1.
27. Hattori, H.; Uryu, T. *J Polym Sci A: Polym Chem* 2000, 38, 887.
28. Zhang, B. Y.; Meng, F. B.; Tian, M.; Xiao, W. Q. *React Funct Polym* 2006, 66, 551.
29. Huang, B.; Ge, J. J.; Li, Y.; Hou, H. *Polymer* 2007, 48, 264.
30. Eleftherios, V. T.; George, P. K. *J Polym Sci Part A: Polym Chem* 1999, 37, 2391.
31. Alexander, L. E. *X-ray Diffraction Methods in Polymer Science*; Wiley: New York, 1969.
32. Jia, Y. G.; Zhang, B. Y.; Sun, Q. J.; Chang, H. X. *Colloid Polym Sci* 2004, 282, 1077.
33. Rousseau, I. A.; Qin, H.; Mather, P. T. *Macromolecules* 2005, 38, 4103.
34. Wang, Y.; Zhang, B.; He, X.; Wang, J. W. *Colloid Polym Sci* 2007, 285, 1077.